




Article

UWB and MB-OFDM for Lunar Rover Navigation and Communication

J. de Curtò ^{1,2,3,*} , I. de Zarzà ^{1,2,3}  and Carlos T. Calafate ¹ 

¹ Departamento de Informática de Sistemas y Computadores, Universitat Politècnica de València, 46022 València, Spain; dezarza@em.uni-frankfurt.de (I.d.Z.); calafate@disca.upv.es (C.T.C.)

² Informatik und Mathematik, GOETHE-University Frankfurt am Main, 60323 Frankfurt am Main, Germany

³ Estudis d'Informàtica, Multimèdia i Telecomunicació, Universitat Oberta de Catalunya, 08018 Barcelona, Spain

* Correspondence: decurto@em.uni-frankfurt.de

Abstract: This paper presents a comprehensive study of ultra-wideband (UWB) and multi-band orthogonal frequency-division multiplexing (MB-OFDM) technologies for lunar rover navigation and communication in challenging terrains. Lunar missions pose unique challenges, such as signal propagation in the lunar environment, terrain elevation, and rover movement constraints. To address these challenges, we propose a hybrid communication and navigation system that leverages UWB technology for high-precision positioning and MB-OFDM for robust and high-throughput communication. We develop a realistic simulation framework that incorporates terrain elevation, obstacles, and rover movement constraints, along with a simple fading model for communication. Simulation results demonstrate the effectiveness of the proposed system in navigating lunar rovers to their target locations while maintaining reliable communication links with a lunar lander. A novel approach based on game theory for rover navigation is also presented. The study provides valuable insights into the design and optimization of communication and navigation systems for future lunar missions, paving the way for seamless integration of advanced terrestrial technologies in extraterrestrial environments.

Keywords: UWB; MB-OFDM; lunar missions; interplanetary communications; game theory; rover

MSC: 94A12; 93C85; 85-10; 91A40



Citation: de Curtò, J.; de Zarzà, I.; Calafate, C.T. UWB and MB-OFDM for Lunar Rover Navigation and Communication. *Mathematics* **2023**, *11*, 3835. <https://doi.org/10.3390/math11183835>

Academic Editors: Camelia Petrescu and Valeriu David

Received: 18 August 2023

Revised: 30 August 2023

Accepted: 5 September 2023

Published: 7 September 2023



Copyright: © 2023 by the authors. Licensee MDPI, Basel, Switzerland. This article is an open access article distributed under the terms and conditions of the Creative Commons Attribution (CC BY) license (<https://creativecommons.org/licenses/by/4.0/>).

1. Introduction and Overview

The exploration of the Moon has gained renewed interest in recent years, fueled by ambitious missions from both governmental and private space agencies. These lunar missions aim to establish a permanent human presence, exploit resources, and conduct scientific research. A key aspect of lunar missions is the deployment and operation of rovers, which play a crucial role in the exploration and utilization of the lunar surface. Ensuring reliable and efficient navigation and communication systems for these rovers is of paramount importance for the success of such missions.

Ultra-wideband (UWB) [1–4] technology has emerged as a promising candidate for high-precision positioning and navigation due to its fine time resolution and ability to operate in cluttered environments. Meanwhile, multi-band orthogonal frequency-division multiplexing (MB-OFDM) [5,6] has been demonstrated as an effective communication technique, offering high data rates and robustness against interference and multipath propagation. The integration of UWB and MB-OFDM technologies can provide a comprehensive solution for lunar rover navigation and communication challenges.

In this paper, we investigate the application of UWB and MB-OFDM technologies for lunar rover operations [7–9]. We develop a realistic simulation framework that incorporates

various lunar environment factors, such as terrain elevation, obstacles, and rover movement constraints. The framework also considers the signal propagation characteristics of the lunar environment and incorporates a simple fading model to simulate communication links between rovers and a lunar lander. Through simulations, we demonstrate the effectiveness of the proposed hybrid system in navigating lunar rovers to their target locations while maintaining reliable communication links [10,11]. A technique for rover navigation based on game theory is provided.

The remainder of this paper is organized as follows: Section 2 introduces the main considerations regarding designing a communication network on the Moon. Section 3 provides a brief overview of UWB and MB-OFDM technologies, along with their potential applications in lunar missions. Section 3.2 presents a comparison between UWB technology and THz communication technologies in the context of 5G. Section 4 describes the simulation framework and the various factors considered in modeling the lunar environment, presents the simulation results, and provides a detailed performance analysis of the proposed system. Section 5 discusses an approach based on game theory for rover navigation. Finally, Section 6 concludes the paper and provides potential directions for future research.

2. Lunar Communications: Network Topology and Frequency Bands

Designing a lunar communication network requires considering coverage, latency, and redundancy. In this simplified scenario, we propose a hybrid network consisting of satellite relays and surface infrastructure. Figure 1 shows an illustration of this hybrid architecture, which consists of lunar base stations, orbiting satellites, and Earth-based stations.

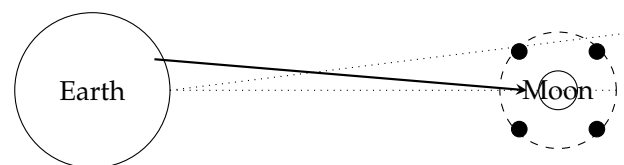


Figure 1. Hybrid lunar communication network architecture with satellite relays and surface infrastructure. This diagram shows Earth, the Moon, a lunar base station, and orbiting satellites. The dashed circle represents satellite orbits, while the filled circles on the orbit represent individual satellites. The dotted lines indicate communication links between Earth, the lunar base station, and the satellites. The FSOC link between Earth and the Moon is represented by a thick arrow.

To provide context for our assumptions and calculations, we present some essential data related to the Moon and its communication with Earth. The Moon's circumference is about 10,921 km, and the average Earth–Moon distance is 384,400 km. In our proposed architecture, we assume that the lunar base and relay satellites have a communication range of 500 km. With N satellites, 11 are needed for full coverage. These satellites can be placed in circular equatorial or polar orbits to ensure continuous coverage. Optical communication systems, such as laser-based free space optical communication (FSOC), can provide high-speed, low-latency communication between Earth and the Moon. In our analysis, we assume that the FSOC system has a data rate of 10 Gbps. Our calculations show a one-way latency of 1.28 s and an 800 s (13.3 min) transmission time for a 1 TB file.

To select suitable frequency bands for lunar communication, we must consider interference potential and Earth-based network compatibility. We examine the S-band (2–4 GHz), X-band (8–12 GHz), and Ka-band (26.5–40 GHz), used for satellite communication. Lower frequency bands offer longer communication ranges but lower data rates, while higher frequency bands support higher data rates but experience higher signal attenuation. In conclusion, lower frequency bands like the S-band may be used for basic communication, while higher frequency bands like the X-band and Ka-band can be used for high-resolution imagery, video communication, and data-intensive applications.

For the lunar surface communication, we focus on the integration of UWB and MB-OFDM technologies. These technologies enable high data rates and precise positioning, facilitating rover navigation and communication in the challenging lunar terrain. In the

following sections, we will delve into the details of the UWB and MB-OFDM systems and their implementation in the lunar environment.

Designing an optimal network topology for lunar communications involves considering multiple factors, including coverage, latency, and redundancy. In this example, we focus on a simple scenario to illustrate the concepts involved. We propose a hybrid network topology that combines satellite-based relay systems and surface-based communication infrastructure.

Assumptions: The Moon's circumference is approximately 10,921 km. The lunar base and relay satellites have a communication range of 500 km on the lunar surface. There are N satellites in orbit providing coverage for the lunar surface. Based on the developed code and the given assumptions, 11 satellites are required for full coverage of the lunar surface. This means that, at any given time, there will be a satellite within communication range (500 km) of any point on the Moon's surface. In reality, achieving full coverage can be more complex due to factors like the Moon's uneven topography and signal attenuation caused by the lunar regolith, but for the sake of this example, we are using a simplified model. To elaborate on the concept, these 11 satellites would be placed in strategically chosen orbits to ensure continuous communication coverage. To achieve this, the satellites could be placed in a constellation configuration, which could involve:

- Circular equatorial orbits: The satellites are placed in circular orbits around the Moon's equator, evenly spaced in terms of longitude. This configuration provides continuous coverage, as each satellite would cover a specific region of the lunar surface, and their combined coverage would span the entire Moon;
- Polar orbits: The satellites are placed in orbits that pass over or near the Moon's poles. This configuration can also provide continuous coverage, especially when considering the elliptical or inclined nature of the orbits, which can help to optimize coverage for regions near the poles or at higher latitudes.

Optical communication systems, such as laser-based systems, can provide high-speed, low-latency communication between the Moon and Earth. These systems rely on modulating light signals, often in the infrared spectrum, to transmit data. Let us consider the free space optical communication (FSOC) system for this example, as it is a promising technology for such applications.

Assumptions: The average distance between the Moon and Earth is approximately 384,400 km. The speed of light in a vacuum is approximately 299,792 km/s. We will assume a data rate of 10 gigabits per second (Gbps) for the FSOC system. Based on the developed code and the given assumptions, we calculated the one-way latency and the time required to transmit a 1 TB file using the free space optical communication (FSOC) system for communication between the Moon and Earth. The one-way latency of 1.28 s represents the time it takes for a signal to travel from the Moon to Earth, or vice versa, using the optical communication system. This is the minimum amount of time required for a message to be transmitted between the two points, not taking into account any additional processing delays, encoding, or error correction. This low-latency communication is beneficial for time-sensitive operations and real-time control of lunar assets, as it allows for near-instantaneous exchange of information. The calculated time of 800 s (approximately 13.3 min) to transmit a 1 TB file represents a high data rate of 10 Gbps. This high data rate allows for the efficient transmission of large volumes of data, which is crucial for lunar missions that generate significant amounts of scientific data or require high-resolution imagery and video communication. By using FSOC systems, data can be sent back to Earth rapidly, enabling timely analysis and decision making.

To study suitable frequency bands and spectrum allocation strategies for lunar communication systems, we need to consider factors like the potential for interference and compatibility with Earth-based networks. Radio frequency (RF) bands are typically divided into low, medium, and high frequency ranges. Lower frequency bands can penetrate obstacles and provide longer communication ranges, while higher frequency bands can support higher data rates but are more susceptible to signal attenuation.

Let us start by looking at some popular frequency bands used for space communication and their respective characteristics:

- The S-band (2–4 GHz) is commonly used for near-Earth satellite communication, including navigation and weather satellites. It offers moderate data rates and has relatively low signal attenuation;
- The X-band (8–12 GHz) is used for deep space communication, including Mars missions and deep space probes. It provides higher data rates than the S-band, but it is more susceptible to signal attenuation due to its higher frequency;
- The Ka-band (26.5–40 GHz) offers high data rates and is used for high-capacity satellite communication systems. However, it is more susceptible to signal attenuation caused by atmospheric conditions, such as rain.

The calculated free space path loss (FSPL) for each frequency band provides insight into the signal attenuation that occurs over the average Moon–Earth distance. FSPL represents the loss in signal power that results solely from the spreading of the electromagnetic wave as it travels through free space. The greater the FSPL is, the more significant the signal attenuation over the given distance will be. Here are the calculated FSPL values for each frequency band: S-band—212.10 dB, X-band—224.14 dB, and Ka-band—234.24 dB. These results indicate that signal attenuation increases with frequency. The S-band experiences the lowest FSPL, while the Ka-band experiences the highest. Lower frequency bands, such as the S-band, are generally more resistant to signal attenuation and can penetrate obstacles more easily, providing longer communication ranges. However, they typically support lower data rates compared to higher frequency bands. Higher frequency bands, such as the X-band and Ka-band, can support higher data rates, which is essential for applications that require the transmission of large volumes of data. However, these bands are more susceptible to signal attenuation, as demonstrated by their higher FSPL values. Additionally, they may experience higher levels of interference due to atmospheric conditions, such as rain.

When selecting a frequency band for lunar communication systems, it is crucial to balance the need for data rate capacity and signal strength. Lower frequency bands, like the S-band, may be suitable for basic communication and telemetry, while higher frequency bands, like the X-band and Ka-band, can be used for high-resolution imagery, video communication, and data-intensive scientific applications.

2.1. Overview of Lunar Missions

An understanding of the general architecture of lunar missions is essential for appreciating the specific challenges and solutions addressed in this paper. Figure 2a presents an overview of a typical lunar mission, while Figure 2b shows a common visual illustration.

In a standard mission, a lunar lander transports one or more rovers to the lunar surface. Upon landing, the rovers are deployed to carry out various tasks, such as scientific investigations or logistical operations. The lander often serves as a relay point for communication between the rovers and Earth-based stations. The critical role of navigation and communication systems, such as UWB and MB-OFDM, is evident in ensuring the success of such complex missions [12–14].

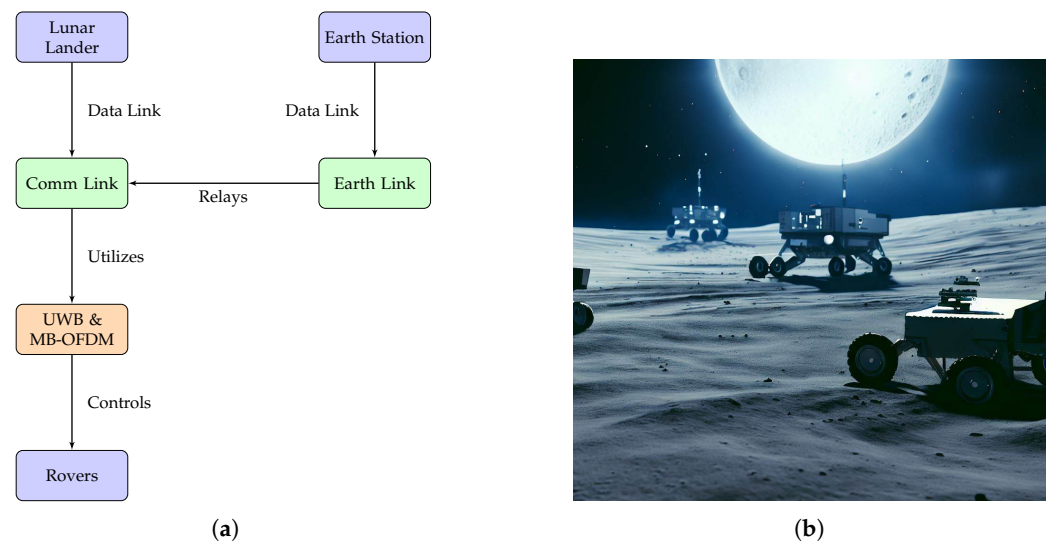


Figure 2. Diagram and visual illustration of a typical lunar mission. (a) General diagram illustrating the components and architecture of a typical lunar mission. (b) Visual illustration of the setup with a lander communicating with several rovers.

2.2. Motivation for Employing UWB and MB-OFDM in Lunar Rover Navigation

UWB and MB-OFDM are pivotal technologies for achieving robust and high-throughput communication between lunar rovers and the lunar lander. These technologies were chosen due to their unique advantages in the context of lunar exploration. Below, we outline the contributions of each:

UWB

- **High data rate:** UWB can provide extremely high data rates, crucial for transmitting high-definition sensor data;
- **Low power consumption:** UWB's low-power spectral density makes it energy-efficient, prolonging the mission lifespan;
- **Robustness:** UWB is known for its robustness against multi-path fading and interference, which is critical in challenging lunar terrains.

MB-OFDM

- **Spectral efficiency:** MB-OFDM is highly spectral efficient, making the best use of available frequency bands;
- **Flexibility:** It allows flexible allocation of resources, which can be dynamically adjusted based on mission requirements;
- **Resilience:** The technology is resilient to frequency-selective fading, making it ideal for lunar operations.

The integration of UWB and MB-OFDM technologies with the pathfinding algorithm forms one of the cornerstones of this research study. These communication technologies provide the backbone that supports the decision-making capabilities of the pathfinding algorithm and one of the key components of the game-theoretic proposal, enabling rovers to make more informed choices based on real-time data.

- **Data transmission:** High-speed data transmission enabled by UWB and MB-OFDM ensures that the rovers can receive timely updates, essential for the pathfinding algorithm to operate optimally;
- **Scalability:** The adaptability of MB-OFDM supports the operation of multiple rovers, thereby allowing the pathfinding algorithm to scale its operations;
- **Reliability:** The robustness of UWB ensures that essential control messages, crucial for the pathfinding algorithm, are delivered reliably even in the harshest of conditions.

3. UWB and MB-OFDM

UWB [15] is a radio technology that utilizes a large portion of the radio spectrum, typically exceeding 500 MHz, for the transmission of low-power, short-range signals. The key advantage of UWB is its high time resolution, which enables precise positioning and navigation capabilities. The impulse radio nature of UWB allows it to penetrate obstacles and operate effectively in cluttered environments, making it suitable for lunar missions [16].

UWB signals are characterized by their large fractional bandwidth, given by: $B_f = (f_H - f_L) / f_c$, where f_H and f_L are the highest and lowest frequencies of the UWB signal, respectively, and f_c is the center frequency. According to the Federal Communications Commission (FCC), a signal is considered UWB if its fractional bandwidth is greater than 0.2 or its bandwidth is greater than 500 MHz.

The time difference of arrival (TDoA) method is commonly employed for UWB-based positioning systems. The TDoA measures the difference in arrival times of UWB signals transmitted from multiple anchors to a receiver. By calculating the TDoA values for at least three anchors, the receiver can accurately determine position using trilateration.

A key feature of UWB signals is their extremely short duration, often in the order of nanoseconds. These signals are generated by transmitting a series of pulses with a very low duty cycle, resulting in a wide bandwidth and minimal interference with other narrowband systems. The mathematical representation of a UWB pulse is given by:

$$p(t) = A \cdot \text{rect}\left(\frac{t - t_0}{T_p}\right) \cdot \cos(2\pi f_c(t - t_0)), \tag{1}$$

where A is the amplitude, t_0 is the pulse start time, T_p is the pulse duration, and f_c is the carrier frequency. The rect function is defined as:

$$\text{rect}(x) = \begin{cases} 1, & \text{if } -\frac{1}{2} \leq x \leq \frac{1}{2}, \\ 0, & \text{otherwise.} \end{cases} \tag{2}$$

The wide bandwidth of UWB signals offers several advantages, including high data rates, precise time resolution, and robustness against multipath fading and interference [16,17]. Moreover, UWB systems can coexist with other wireless technologies without causing significant interference, making them suitable for various applications, such as indoor positioning, radar systems, and wireless personal area networks [18,19].

The UWB channel can be modeled as a linear time-variant system with multipath components, each characterized by its path gain, delay, and phase shift. The impulse response of the UWB channel is given by:

$$h(t, \tau) = \sum_{z=1}^{N_p} \alpha_z(t) \cdot \delta(\tau - \tau_z(t)) \cdot e^{-j\phi_z(t)}, \tag{3}$$

where N_p is the number of multipath components, $\alpha_z(t)$ is the path gain, $\tau_z(t)$ is the delay, $\phi_z(t)$ is the phase shift, and $\delta(\cdot)$ is the Dirac delta function. The received UWB signal, $r(t)$, is obtained by convolving the transmitted signal, $s(t)$, with the channel impulse response:

$$r(t) = s(t) * h(t, \tau) + n(t), \tag{4}$$

where $n(t)$ is the additive white Gaussian noise (AWGN) with zero mean and variance σ^2 . To recover the transmitted signal, a UWB receiver typically employs a matched filter or a rake receiver that combines the energy from different multipath components.

3.1. UWB Positioning Techniques

UWB technology is particularly well suited for positioning and localization applications owing to its high time resolution and ability to resolve multipath components. Some common UWB-based positioning techniques include time of arrival (ToA), time difference

of arrival (TDoA), and angle of arrival (AoA). These techniques rely on accurate estimation of the propagation delay or angle of arrival of the UWB signal, which can be achieved using cross-correlation or maximum likelihood estimation methods.

ToA is a technique that estimates the distance between a transmitter and a receiver by measuring the time it takes for a UWB signal to travel from the transmitter to the receiver. The distance d can be calculated using the relation: $d = c \cdot t_{\text{prop}}$, where c is the speed of light and t_{prop} is the propagation time of the UWB signal. ToA-based positioning typically requires the transmitter and receiver to be synchronized, and the accuracy of the distance estimation is directly proportional to the UWB signal's time resolution.

TDoA is a technique that measures the difference in arrival times of a UWB signal at multiple receivers. The position of the transmitter can be estimated by finding the intersection of hyperbolic curves obtained from the time difference measurements. TDoA-based positioning does not require the transmitter and receiver to be synchronized but demands precise time synchronization among the receivers.

AoA is a technique that estimates the transmitter's position by measuring the angle at which the UWB signal arrives at multiple receivers. The position of the transmitter can be estimated by finding the intersection of the lines obtained from the angle measurements. AoA-based positioning typically requires an array of antennas at the receiver to measure the angle of arrival accurately.

3.2. Comparison of UWB and B5G

This section presents a comparative study of the performance of UWB and a specific Beyond 5G technology, focusing on key performance indicators such as latency, data rate, path loss, and distance. To provide a relevant comparison, we consider terahertz (THz) communication [20], which offers ultra-high data rates and low latency. THz communication has been proposed as a promising candidate for Beyond 5G networks, particularly for short-range and high-capacity applications. UWB offers the benefits of high-precision positioning, robustness against multipath fading and interference, and coexistence with other wireless technologies, while THz communication provides ultra-high data rates and low latency.

3.2.1. Latency vs. Distance and Data Rate vs. Distance

Latency is a critical factor in lunar communication systems, as it affects the responsiveness and coordination of rovers, landers, and other nodes in the network. The latency in both UWB and Beyond 5G systems can be modeled as a function of the distance between the transmitter and receiver, taking into account the propagation speed, the processing delay, and the queuing delay.

$$\text{Latency} = \frac{\text{Distance}}{c} + \text{Processing Delay} + \text{Queuing Delay}, \quad (5)$$

where c represents the speed of light in a vacuum.

UWB technology exhibits lower latency as the distance increases within its short-range operating limits owing to its ultra-wide bandwidth and impulse-based transmission. In contrast, Beyond 5G [20] systems may experience higher latency due to the increased overhead from the complex modulation and coding schemes employed to achieve higher data rates. It is important to note that the UWB technology is suitable for short-range communication scenarios (e.g., within a lunar base or between closely spaced rovers), while Beyond 5G technology can be more suitable for longer range communications. The data rate of a communication system is a crucial aspect of its performance, particularly when transmitting large amounts of data, such as high-resolution images and scientific measurements. In UWB systems, the data rate is primarily determined by the available bandwidth and the modulation scheme employed. The Shannon–Hartley theorem, which states the maximum achievable data rate for a given bandwidth and signal-to-noise ratio

(SNR), can provide a rough estimate of the data rate. However, it should be noted that this equation is a theoretical upper bound.

$$\text{Data Rate} = B \times \log_2(1 + \text{SNR}), \tag{6}$$

where B represents the bandwidth and SNR denotes the signal-to-noise ratio. On the other hand, Beyond 5G systems leverage advanced techniques, such as massive multiple-input and multiple-output (MIMO) and beamforming, to achieve high data rates over longer distances. These techniques help improve the SNR, allowing for higher data rates without necessarily increasing the available bandwidth. Our simulation results indicate that Beyond 5G systems can achieve higher data rates compared to UWB, particularly at longer distances. However, this comes at the cost of increased complexity and power consumption, which may be detrimental in the resource-constrained lunar environment.

3.2.2. Path Loss vs. Distance

Path loss is a significant factor in determining the signal strength and communication range in wireless systems. In both UWB and Beyond 5G technologies, path loss can be modeled using the log-distance path loss model:

$$\text{Path Loss (dB)} = PL_{d_0} + 10n \log_{10}\left(\frac{d}{d_0}\right), \tag{7}$$

where PL_{d_0} represents the reference path loss at distance d_0 , n is the path loss exponent, and d is the distance between the transmitter and receiver.

UWB systems exhibit lower path loss over short distances due to their wide bandwidth and impulse-based transmission, as depicted in Figure 3. In contrast, Beyond 5G systems may experience higher path loss, especially in the presence of obstacles and multipath propagation. However, advanced techniques, such as beamforming and massive MIMO, can help mitigate these effects.

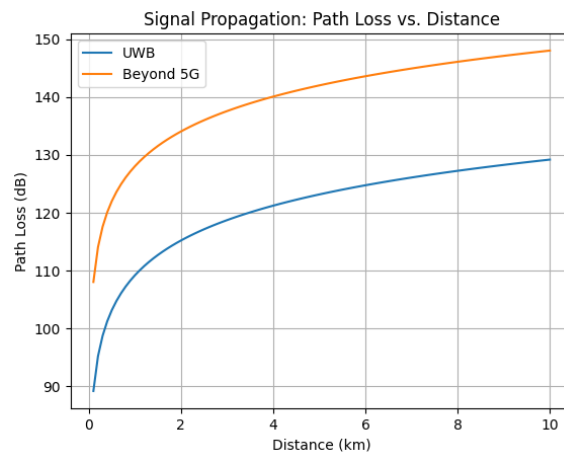


Figure 3. Path loss vs. distance comparison using UWB and B5G.

3.3. MB-OFDM

OFDM [21,22] is widely used in modern communication systems for its robustness against multipath fading and inter-symbol interference. OFDM divides the available frequency band into multiple closely-spaced orthogonal subcarriers, each carrying a modulated data symbol. Multi-band OFDM (MB-OFDM) extends the basic OFDM concept by dividing the available spectrum into several non-overlapping frequency bands, each containing a group of OFDM subcarriers. This approach provides better spectral efficiency, and allows for dynamic frequency allocation to accommodate varying communication requirements. The total number of subcarriers in an MB-OFDM system is given by:

$N_{total} = N_{bands} * N_{subcarriers_per_band}$, where N_{bands} is the number of frequency bands and $N_{subcarriers_per_band}$ is the number of OFDM subcarriers within each band.

In OFDM, the orthogonality of the subcarriers allows them to be closely spaced, resulting in efficient bandwidth utilization. The time-domain OFDM signal can be represented as:

$$s(t) = \sum_{o=0}^{N-1} \text{Re}\left(X_o e^{j2\pi o \Delta f t}\right), \quad (8)$$

where N is the number of subcarriers, Δf is the subcarrier spacing, X_o is the complex data symbol for the o -th subcarrier, and t is time.

In MB-OFDM, each band consists of several orthogonal subcarriers, and data are transmitted by frequency hopping across these bands. This approach provides increased robustness against narrowband interference and improves spectral efficiency by allowing the system to adapt to varying channel conditions. The time-domain MB-OFDM signal can be represented as:

$$s(t) = \sum_{n=0}^{M-1} \sum_{o=0}^{N-1} \text{Re}\left(X_{n,o} e^{j2\pi(n\Delta f_b + o\Delta f)t}\right), \quad (9)$$

where M is the number of bands, Δf_b is the band spacing, and $X_{n,o}$ is the complex data symbol for the o -th subcarrier in the n -th band.

3.3.1. Subcarrier Modulation and Demodulation

Data symbols are modulated onto the subcarriers using a variety of modulation schemes, such as binary phase-shift keying (BPSK), quadrature phase-shift keying (QPSK), or quadrature amplitude modulation (QAM). The choice of modulation scheme depends on the desired trade-off between data rate, power consumption, and error performance. Demodulation is performed using the inverse process, which typically involves fast Fourier transform (FFT) operations to convert the received time-domain signal into frequency-domain data.

3.3.2. Channel Estimation and Equalization

Channel estimation and equalization techniques are employed in MB-OFDM systems to compensate for the effects of channel impairments, such as multipath fading and frequency-selective fading. Common methods for channel estimation include pilot symbol-assisted estimation and decision-directed estimation. Equalization techniques, such as zero forcing (ZF) or minimum mean square error (MMSE) equalizers, are applied to mitigate the effects of channel distortions. In summary, MB-OFDM technology combines the advantages of OFDM with frequency hopping across multiple bands, resulting in improved spectral efficiency and robustness against narrowband interference.

3.4. Theoretical Analysis of RF Interference between UWB and MB-OFDM

RF interference between UWB and MB-OFDM systems poses a critical concern in the implementation of hybrid communication and navigation systems for lunar rovers. In this section, we present a theoretical framework that analyzes this potential interference and discuss possible mitigation techniques.

The key metrics that determine the extent of RF interference are:

1. Spectral overlap: frequency ranges where both UWB and MB-OFDM operate;
2. Signal-to-interference ratio (SIR): measures the strength of the desired signal relative to interference;
3. Adjacent channel leakage ratio (ACLR): represents power leakage into adjacent frequency bands.

Let $P_{\text{UWB}}(f)$ and $P_{\text{MB-OFDM}}(f)$ represent the power spectral densities of the UWB and MB-OFDM systems, respectively. Then, the interference I can be modeled as:

$$I = \int_{-\infty}^{\infty} P_{\text{UWB}}(f) \cdot P_{\text{MB-OFDM}}(f) df \quad (10)$$

For an acceptable level of operation, I should be below a certain threshold I_{max} .

Potential mitigation strategies:

1. Dynamic frequency selection (DFS): assign non-overlapping frequency bands when possible;
2. Power control: adjust the transmission power based on the proximity of interfering signals;
3. Time division multiple access (TDMA): allocate distinct time slots for UWB and MB-OFDM signals.

The theoretical analysis indicates that careful system design, accounting for interference, can enable effective coexistence of UWB and MB-OFDM systems in lunar rover applications.

3.5. Potential Applications in Lunar Missions

The integration of UWB and MB-OFDM technologies provides a comprehensive solution for both navigation and communication in lunar rover operations. By combining the high data rates, precise positioning, and reliable communication offered by UWB and MB-OFDM, the resulting system is highly adaptable to varying channel conditions and challenging environments, such as lunar missions. The use of multiple bands and orthogonal subcarriers enables efficient utilization of the available spectrum, while the inherent robustness against multipath fading and narrowband interference ensures reliable communication links. The high data rates provided by the MB-OFDM UWB system are suitable for transmitting large amounts of information, such as high-resolution images, video streams, and scientific data. Furthermore, the precise positioning capabilities enabled by UWB can assist in navigation and coordination among lunar rovers, landers, and other communication nodes.

Incorporating these technologies in tandem allows for a flexible and reliable communication and navigation system that is well suited to the challenging lunar environment. UWB can provide high-precision positioning and navigation capabilities, enabling rovers to accurately traverse the lunar surface and reach target locations. Simultaneously, MB-OFDM can offer robust communication links, ensuring efficient information exchange between rovers and the lunar lander or other infrastructure. Overall, the integration of UWB and MB-OFDM technologies offers significant advantages for lunar missions, fostering the development of an advanced communication and navigation system for lunar rovers that can effectively navigate and operate in the complex lunar terrain.

4. Simulation Framework and Lunar Environment Modeling

The simulation framework developed in this work (code is available at: <https://doi.org/10.24433/CO.5122707.v1>, accessed on 1 August 2023) aims to model the behavior of rovers in the lunar environment, focusing on their navigation and communication capabilities. The framework incorporates terrain generation using PERLIN noise, obstacle placement, rover movement, and communication system modeling, including UWB and OFDM technologies to illustrate the applicability of MB-OFDM.

The main components of the simulation framework are:

- Terrain generation using PERLIN noise: a grid-based representation of the lunar surface with varying elevation levels;
- Obstacle placement: random placement of obstacles on the terrain representing rocks and other surface features;
- Rover movement: modeling rover movement based on navigation algorithms, such as A* pathfinding or reinforcement learning (RL) techniques like proximal policy optimization (PPO) [23], considering constraints like terrain elevation and slope;

- Communication system: incorporating UWB positioning, OFDM communication, and simple fading models to estimate signal strength and communication delay.

The A* pathfinding algorithm [24] is an informed search algorithm that efficiently finds the shortest path between a given start and end point in a weighted graph, such as a grid or a graph representing a terrain. It is widely used in various applications, including robotics, video games, and route planning, due to its effectiveness and performance. The A* algorithm combines the benefits of Dijkstra's algorithm, which guarantees the shortest path, and the greedy best-first-search algorithm, which directs the search towards the goal using a heuristic function.

Given a graph $G = (V, E)$, where V is the set of vertices (nodes) and E is the set of edges, let s be the starting node and g be the goal node. The algorithm maintains two sets of nodes, an open set O and a closed set C . The open set initially contains the starting node, while the closed set is initially empty. Each node $n \in V$ is associated with two cost values: the actual cost $g(n)$, representing the cost of the path from the starting node to n , and the estimated total cost $f(n)$, which is the sum of $g(n)$ and a heuristic function $h(n)$ that estimates the cost from n to the goal node g :

$$f(n) = g(n) + h(n). \quad (11)$$

The A* algorithm performs the steps until the goal node is reached or the open set is empty. The heuristic function $h(n)$ plays a crucial role in the performance of the A* algorithm. A good heuristic function should be admissible, meaning it never overestimates the actual cost to reach the goal. A common choice for grid-based graphs is the Euclidean distance or the Manhattan distance. The choice of the heuristic function depends on the problem domain and the constraints imposed by the specific application. Upon termination of the algorithm, if the goal node is reached, the optimal path can be reconstructed by traversing the parent pointers from the goal node to the starting node, in reverse order. If the open set is empty and the goal node is not reached, it implies that there is no valid path between the start and goal nodes. Algorithm 1 illustrates the main steps.

Algorithm 1 A* Pathfinding Algorithm

- 1: Initialize open set O with the starting node s and closed set C as empty
 - 2: **while** O is not empty **do**
 - 3: Select the node n from the open set O with the lowest estimated total cost $f(n)$ and remove it from O
 - 4: **if** n is the goal node g **then**
 - 5: Reconstruct the optimal path and terminate the algorithm
 - 6: **end if**
 - 7: Add n to the closed set C
 - 8: **for** each neighbor m of n that is not in the closed set C **do**
 - 9: Calculate the tentative cost for m , $g_t(m) = g(n) + c(n, m)$, where $c(n, m)$ is the cost of moving from n to m
 - 10: **if** m is not in the open set O or $g_t(m) < g(m)$ **then**
 - 11: Set $g(m) = g_t(m)$
 - 12: Calculate the estimated total cost for m , $f(m) = g(m) + h(m)$
 - 13: Set the parent of m to n
 - 14: **if** m is not in the open set O **then**
 - 15: Add m to O
 - 16: **end if**
 - 17: **end if**
 - 18: **end for**
 - 19: **end while**
-

4.1. Lunar Environment Modeling

Several factors were considered to model the lunar environment accurately and assess the performance of the proposed navigation and communication system. These factors included:

- Terrain elevation: A randomly generated elevation map was created to simulate the uneven lunar surface. Elevation differences impact rover movement and navigation due to slope constraints;
- Obstacle placement: Obstacles in the lunar environment, such as rocks and craters, affect rover navigation and communication. The simulation framework places random obstacles on the terrain and validates rover movement to avoid collisions;
- Rover movement constraints: Rovers on the lunar surface are subject to movement constraints, such as maximum slope and velocity limits. These constraints were incorporated into the simulation framework to ensure realistic rover behavior;
- Communication models: The integration of UWB positioning and MB-OFDM communication, along with a simple fading model, provides a comprehensive communication system for the lunar rovers. These models were employed to estimate communication delay and signal strength between the rovers and the lunar lander.

In Figure 4, we show a conceptual plot of a lander acting as an anchor and communicating with several rovers that are exploring the terrain.

Rover and Lander Positions and Communication Links

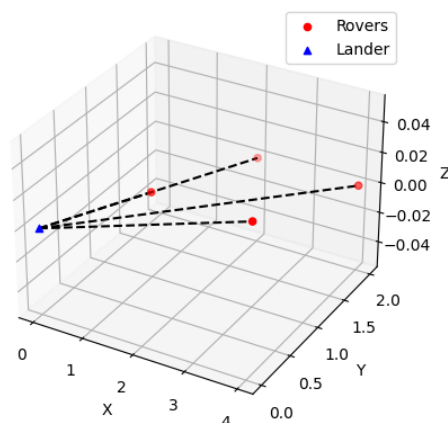


Figure 4. Three-dimensional (3D) representation of a lander acting as anchor and communicating to several rovers.

4.2. Simulation Parameters

To provide a comprehensive evaluation of the proposed system, we consider a set of realistic parameters for UWB, MB-OFDM, terrain generation, and rover movement constraints. For instance, Table 1 provides good default parameters for the simulations.

The parameters were chosen based on a balance between real-world feasibility and the need for extensive simulation testing. The selected parameter values provide a robust testbed for evaluating the system's performance in a lunar environment [25].

Table 1. Summary of good default simulation parameters.

Parameter Category	Parameter	Value
UWB	Frequency range	3.1–10.6 GHz
	Bandwidth	500 MHz
	Modulation scheme	BPSK
	Transmission power	−41.3 dBm/MHz
MB-OFDM	Subcarrier spacing	312.5 kHz
	Number of subcarriers	128
	Modulation scheme	64-QAM
	Bandwidth	20 MHz
Terrain	Noise Scale	0.1
	Octaves	4
	Persistence	0.5
	Lacunarity	2.0
Rover	Maximum speed	0.5 m/s
	Turning radius	0.3 m
	Incline limit	30°

4.3. Simulation Results

The simulation was performed using the developed framework incorporating UWB positioning, OFDM communication, terrain generation using PERLIN noise, and rover movement constraints. The results provide insights into the performance of the proposed system in a realistic lunar environment. Several scenarios were simulated with varying terrain, obstacle placements, and rover-target locations; an example is depicted in Figure 5a,b, where we take into account the elevation of the terrain.

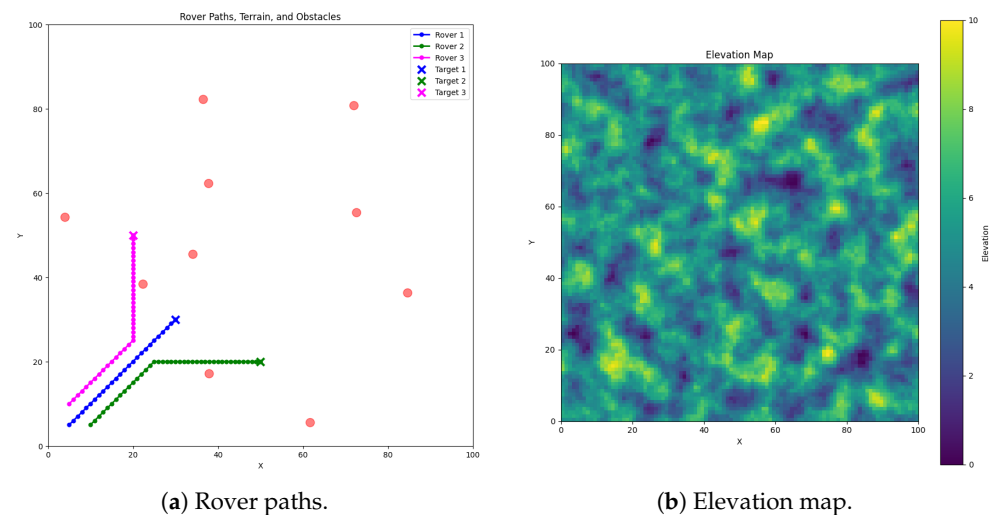


Figure 5. Simulation results. (a) Two-dimensional (2D) representation of a simulated scenario with several rovers following a given path. (b) Corresponding elevation of the terrain for the simulated scenario with PERLIN noise.

The simulation results can be summarized as follows:

- Navigation performance: The rovers were able to navigate to their target locations using the A* pathfinding algorithm, considering terrain elevation, slope constraints, and obstacle avoidance. The generated paths were efficient and safe, ensuring minimal travel time and energy consumption;
- Communication performance: The integrated UWB and OFDM communication system provided reliable and robust communication between the rovers and the lunar lander. The simple fading model allowed for the estimation of signal strength and

communication delay, demonstrating the effectiveness of the proposed system in maintaining connectivity throughout the mission;

- **Robustness and adaptability:** The simulation framework demonstrated the ability to handle various scenarios and environmental conditions, proving the adaptability and robustness of the proposed system in the lunar environment.

Figure 6a shows the relationship between signal strength and the distance between the rover and the lunar lander. This plot provides insight into how the signal strength is affected by the distance traveled by the rover. Figure 6b presents the communication delay as a function of the distance between the rover and the lunar lander, showcasing the effectiveness of the proposed communication system in maintaining connectivity throughout the mission.

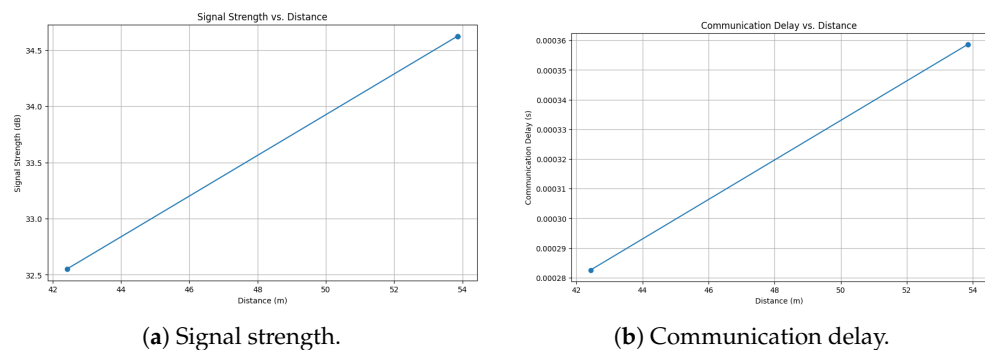


Figure 6. Telecommunication analysis. (a) Signal strength (dB) vs. distance (m) between the rover and the lunar lander. (b) Communication delay (s) vs. distance (m) between the rover and the lunar lander.

Specifically, Figure 6a,b present the telecommunication analysis concerning two key metrics: (a) signal strength in dB vs. distance in meters between the rover and the lunar lander and (b) communication delay in seconds vs. distance in meters between the rover and the lunar lander.

The simulation results in Figure 6a indicate that the signal strength decreases logarithmically with increasing distance between the rover and the lunar lander. This trend is expected due to the path loss experienced by radio signals over distance, especially in the challenging terrain of the lunar surface. The observed behavior is consistent with the Friis transmission equation and the effects of multi-path fading.

The results shown in Figure 6b reveal that the communication delay increases linearly with the distance between the rover and the lunar lander. This is attributable to the increased time-of-flight of signals as the distance expands. Additionally, the lunar terrain, characterized by craters and rocky formations, may introduce additional delays due to the diffraction and reflection of signals.

These findings have significant implications for the operational boundaries within which the rover and the lunar lander need to stay to maintain effective communication. The results support the feasibility of our proposed UWB and MB-OFDM hybrid system for lunar applications within the parameters and constraints assumed in our simulations.

5. Game-Theoretic Approach in Lunar Rover Navigation

Navigational strategies for lunar rovers have, for the longest time, leaned heavily on classical pathfinding algorithms, of which A* is emblematic. These algorithms, while adept at determining the shortest path, may not necessarily account for the multifaceted challenges lunar rovers confront, especially in scenarios involving multiple rovers with overlapping objectives. In this intricate web of objectives, one must consider not just the brevity of the path but also the safety of the rover, its speed, and the quality of its communication with the lander. Game theory, a mathematical study of interactions between

rational decision makers, emerges as a potent tool in this context, furnishing a framework that can encapsulate these various objectives.

In the gamified version of our problem, each lunar rover is conceptualized as a player. Mathematically, given n rovers, our set of players can be denoted as $P = \{p_1, p_2, \dots, p_n\}$. Each player p_o seeks to optimize its reward function $R(p_o)$, which is influenced by its efficiency in reaching its destination, its adherence to safety protocols, and the integrity of its communication with the lander.

Let S represent the strategy space for a rover. Each rover p_o selects a strategy $s \in S$. The strategies can be mathematically represented as a vector, with potential strategies including:

1. s_1 : minimize the Euclidean distance to the target;
2. s_2 : traverse a path that minimizes elevation changes, represented by a function $E(s)$ that gives the elevation change for strategy s ;
3. s_3 : choose a trajectory that optimizes the communication link with the lander, given by a function $C(s)$ that gives the communication quality for strategy s .

Each strategy combination results in a payoff matrix Π , where each element π_{oz} represents the payoff for player o when players select strategies s_o and s_z , respectively. The payoff is a composite function of:

- $T(s)$: time taken to reach the destination;
- $O(s)$: number of close encounters with obstacles or treacherous terrain;
- $C(s)$: communication quality with the lander.

The payoff function for a rover p_o can be represented as:

$$\Pi(p_o, s) = \alpha T(s) + \beta O(s) + \gamma C(s) \tag{12}$$

where α, β , and γ are weights representing the importance of time, safety, and communication, respectively.

A NASH equilibrium in our game is a state s^* such that no player has an incentive to deviate from its current strategy, given the strategies chosen by the other players. Formally, for every player p_i :

$$R(p_o, s^*) \geq R(p_o, s) \quad \forall s \in S \tag{13}$$

This equilibrium ensures that each rover's selected strategy is optimal in the context of the choices made by its peers, as illustrated below.

Proposition 1. *In a two-rover scenario where both rovers have the same reward weights α, β , and γ and they both prioritize safety ($\beta > \alpha, \gamma$), a strategy s that minimizes the number of close encounters with obstacles (i.e., minimizes $O(s)$) will be part of the NASH equilibrium.*

Proof. Given the two rovers p_1 and p_2 , let us assume p_1 chooses strategy s_1 , which minimizes $O(s)$, and p_2 chooses some other strategy s_2 .

From the given conditions, the payoff for p_1 when choosing s_1 is:

$$\Pi(p_1, s_1) = \alpha T(s_1) + \beta O(s_1) + \gamma C(s_1)$$

Since s_1 minimizes $O(s)$ and $\beta > \alpha, \gamma$, $\Pi(p_1, s_1)$ will be greater than the payoff from any other strategy.

For rover p_2 , since $\beta > \alpha, \gamma$, it will also achieve its maximum payoff when it chooses a strategy that minimizes $O(s)$. Thus, the best response for p_2 when p_1 chooses s_1 is to also choose s_1 .

Similarly, if p_2 were to choose s_1 , the best response for p_1 is s_1 .

Therefore, in the defined scenario, both rovers choosing the strategy s_1 that minimizes close encounters with obstacles is a NASH equilibrium. \square

5.1. System Complexity

The proposed system integrating UWB, MB-OFDM, and a game-theoretic approach for lunar rover navigation is inherently complex due to various factors. The computational aspects become particularly intricate when considering the game-theoretic models described above. Each rover, modeled as a player in a game, must solve a multi-objective optimization problem to find its optimal strategy, which itself is a function of the strategies chosen by other rovers. This introduces the need for solving a NASH equilibrium, adding an additional layer of computational burden. Traditional navigational strategies are also supplemented by a rich set of game-theoretic strategies, requiring complex mathematical modeling and solving of payoff matrices to reach an equilibrium state. Communication-wise, UWB and MB-OFDM demand dynamic bandwidth allocation, channel estimation, and interference mitigation, requiring advanced control algorithms. Furthermore, the time-based localization techniques used in UWB contribute additional complexity. Implementation-wise, the system must be robust, lightweight, and energy-efficient, especially considering the harsh conditions of a lunar mission. Despite these complexities, the proposed system aims for a balanced trade-off between performance and operational constraints, ensuring effective lunar exploration.

5.2. Simulation of Simplified Game-Theoretic Approach in Lunar Rover Navigation

To explore the potential advantages of a game-theoretic approach for lunar rover navigation, we implemented a simplified toy example as a case study. This simulation involved multiple rovers in a hypothetical lunar environment and aimed to illustrate the basics of strategy selection and payoff calculations.

The simulation parameters can be seen in Table 2.

Table 2. Simulation parameters for the simplified game-theoretic lunar rover navigation study.

Parameter	Value
Number of players	$N = 3$
Strategy space	$S = \{\text{move forward, turn left, turn right, stay, move diagonally}\}$
Payoff function	$\text{Payoff}(p, s) = \alpha \times T(s) + \beta \times O(s) + \gamma \times C(s)$
Initial weights	$\alpha = 0.4, \beta = 0.3, \gamma = 0.3$

Each rover was implemented as an object possessing attributes for both position and current strategy. Random values were used to approximate real-world metrics such as time efficiency, obstacle avoidance, and communication strength for the purpose of this simplified simulation. The simulation utilized dynamic weights α , β , and γ to model changing priorities in real-world scenarios. For instance, as a rover approaches an obstacle, it might dynamically adjust the weights to favor obstacle avoidance over time efficiency.

The game was simulated for a total of 100 rounds. During each round, each rover independently selected a strategy at random from the strategy space S . The payoffs for the chosen strategies were then calculated, using randomized values as placeholders for the real-world metrics.

The frequency distribution of strategies, as shown in Figure 7, suggests that, in a more deterministic and refined model, we would expect strategies to converge toward a NASH equilibrium. It is important to emphasize that the stochastic elements in this simulation serve primarily as a simplified representation, illustrating the type of sophisticated calculations that would be involved in a complete, real-world model.

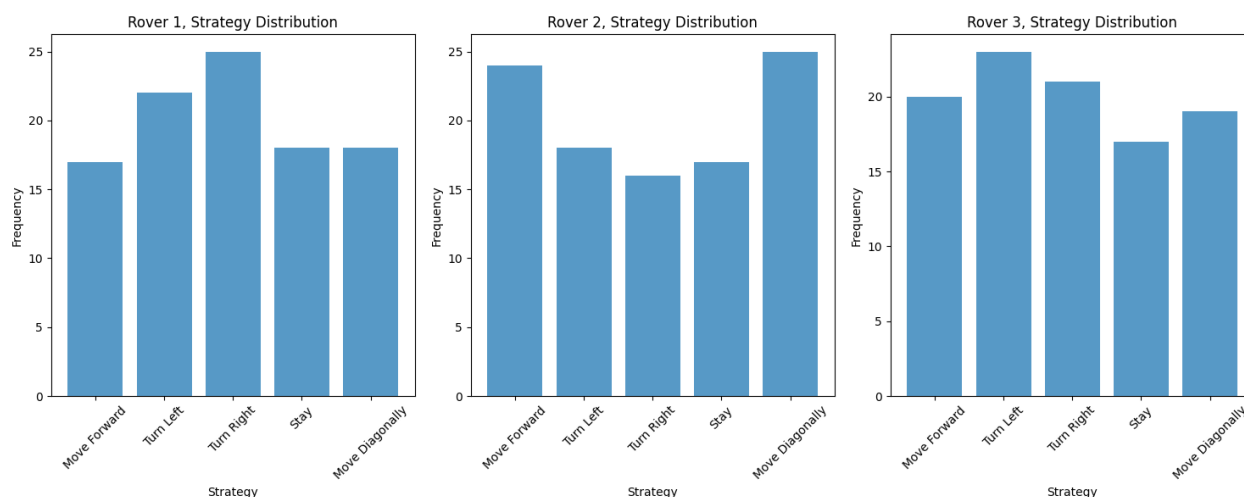


Figure 7. Distribution of strategies in the simplified game-theoretic lunar rover navigation simulation.

6. Conclusions and Future Work

This paper presented a comprehensive simulation framework for evaluating the performance of an integrated UWB and MB-OFDM communication and navigation system in a lunar environment. The framework considered various factors, such as terrain generation, rover movement constraints, obstacle avoidance, and communication channel modeling, to provide a realistic assessment of the proposed system. The simulation results demonstrated the effectiveness and robustness of the integrated UWB and OFDM technologies in ensuring efficient navigation and reliable communication between rovers and the lunar lander. The study's findings have significant implications for the design and deployment of future lunar missions, showcasing the potential of UWB and MB-OFDM technologies in enhancing the capabilities of lunar rovers and landers. Furthermore, the developed simulation framework can be utilized for evaluating other communication and navigation technologies, fostering the development of advanced systems for lunar exploration. Additionally, a novel approach based on game theory for rover navigation was presented.

Future work could focus on:

- Incorporating more complex communication channel models, including multipath effects, to provide a more accurate representation of the lunar environment;
- Investigating the performance of alternative communication and navigation technologies, such as optical or quantum communication systems, in the lunar context;
- Exploring cooperative strategies among multiple rovers for improved navigation, communication, and mission efficiency;
- Further developing the game-theoretic approach, with the possibility of incorporating sophisticated AI techniques for autonomous navigation;
- Evaluating the impact of rover energy consumption, considering the limited power resources available on the Moon, and developing energy-efficient routing and communication algorithms;
- Integrating real-world lunar terrain data and simulating rover missions in specific regions of the Moon to validate the performance of the proposed system under actual lunar conditions.

By addressing these research directions, the presented framework can contribute to the continuous advancement of communication and navigation technologies for lunar exploration, ultimately enabling more efficient and reliable missions on the Moon.

Author Contributions: Conceptualization, J.d.C. and I.d.Z.; funding acquisition, C.T.C.; investigation, I.d.Z. and J.d.C.; methodology, I.d.Z. and J.d.C.; software, J.d.C. and I.d.Z.; supervision, C.T.C.; writing—original draft, J.d.C.; writing—review and editing, C.T.C., J.d.C., and I.d.Z. All authors have read and agreed to the published version of the manuscript.

Funding: We thank the following funding sources from GOETHE-University Frankfurt am Main; “DePP–Dezentrale Planung von Platoons im Straßengüterverkehr mit Hilfe einer KI auf Basis einzelner LKW”, “Center for Data Science & AI”, and “xAIBiology”. We acknowledge the support of R&D project PID2021-122580NB-I00, funded by MCIN/AEI/10.13039/501100011033 and ERDF.

Institutional Review Board Statement: Not applicable.

Informed Consent Statement: Not applicable.

Data Availability Statement: Not applicable.

Conflicts of Interest: The authors declare that they have no conflict of interest. The funders had no role in the design of the study, in the collection, analyses, or interpretation of data, in the writing of the manuscript, or in the decision to publish the results.

Abbreviations

The following abbreviations are used in this manuscript:

Ultra-Wideband	UWB
Multi-Band Orthogonal Frequency-Division Multiplexing	MB-OFDM
Free Space Optical Communication	FSOC
Radio Frequency	RF
Free Space Path Loss	FSPL
Federal Communications Commission	FCC
Time of Arrival	ToA
Time Difference of Arrival	TDoA
Angle of Arrival	AoA
Multiple-Input and Multiple-Output	MIMO
Signal-to-Noise Ratio	SNR
Quadrature Amplitude Modulation	QAM
Binary Phase-Shift Keying	BPSK
Quadrature Phase-Shift Keying	QPSK
Fast Fourier Transform	FFT
Zero Forcing	ZF
Minimum Mean Square Error	MMSE
Reinforcement Learning	RL
Proximal Policy Optimization	PPO

References

1. Aiello, G.R.; Rogerson, G.D. Ultra-wideband wireless systems. *IEEE Microw. Mag.* **2003**, *4*, 36–47. [[CrossRef](#)]
2. Rahayu, Y.; Rahman, T.A.; Ngah, R.; Hall, P. Ultra wideband technology and its applications. In Proceedings of the 2008 5th IFIP International Conference on Wireless and Optical Communications Networks (WOCN '08), Surabaya, Indonesia, 5–7 May 2008; pp. 1–5.
3. Alarifi, A.; Al-Salman, A.; Alsaleh, M.; Alnafessah, A.; Al-Hadhrani, S.; Al-Ammar, M.A.; Al-Khalifa, H.S. Ultra wideband indoor positioning technologies: Analysis and recent advances. *Sensors* **2016**, *16*, 707. [[CrossRef](#)] [[PubMed](#)]
4. Coppens, D.; Shahid, A.; Lemey, S.; Herbruggen, B.V.; Marshall, C.; Poorter, E.D. An overview of UWB standards and organizations (IEEE 802.15.4, FiRa, apple): Interoperability aspects and future research directions. *IEEE Access* **2022**, *10*, 70219–70241. [[CrossRef](#)]
5. Scholtz, R.A. Multiple access with time-hopping impulse modulation. In Proceedings of the MILCOM'93-IEEE Military Communications Conference, Boston, MA, USA, 11–14 October 1993; Volume 2, pp. 447–450.
6. Batra, A.; Balakrishnan, J.; Dabak, A. Multi-band ofdm: A new approach for uwb. In Proceedings of the 2004 IEEE International Symposium on Circuits and Systems (IEEE Cat. No. 04CH37512), Vancouver, BC, Canada, 23–26 May 2004; Volume 5, p. V.
7. Kaiser, T.; Zheng, F.; Dimitrov, E. An overview of ultra-wide-band systems with mimo. *Proc. IEEE* **2009**, *97*, 285–312. [[CrossRef](#)]
8. Chen, T.; Govindaraj, S.; Noel, T.; Welch, C.; Zhang, T. Beacon-based localization of the robot in a lunar analog environment. In Proceedings of the 2020 Chinese Control And Decision Conference (CCDC), Hefei, China, 22–24 August 2020; pp. 4297–4304.
9. Matthies, L.; Kennett, A.; Kerber, L.; Fraeman, A.; Anderson, R.C. Prospects for very long-range mars rover missions. In Proceedings of the 2022 IEEE Aerospace Conference (AERO), Big Sky, MT, USA, 5–12 March 2022; pp. 1–11.
10. Allan, M.; Wong, U.; Furlong, P.M.; Rogg, A.; McMichael, S.; Welsh, T.; Chen, I.; Peters, S.; Gerkey, B.; Quigley, M.; et al. Planetary rover simulation for lunar exploration missions. In Proceedings of the 2019 IEEE Aerospace Conference, Big Sky, MT, USA, 2–9 March 2019; pp. 1–19.

11. Zhang, Z.B.; Zuo, W.; Zeng, X.G.; Gao, X.Y.; Ren, X. The Scientific Data and Its Archiving from Chang'e 4 Mission. In Proceedings of the 4th Planetary Data Workshop, Flagstaff, Arizona, 18–20 June 2019; Volume 2151, p. 7032.
12. Sravya, R.S.; Sreeja, S. Design and simulation of interplanetary lunar rover. *Mater. Today Proc.* **2023**, *in press*. [[CrossRef](#)]
13. Daftry, S.; Chen, Z.; Cheng, Y.; Tepsuporn, S.; Khattak, S.; Matthies, L.; Coltin, B.; Naal, U.; Ma, L.M.; Deans, M. LunarNav: Crater-based Localization for Long-range Autonomous Lunar Rover Navigation. In Proceedings of the 2023 IEEE Aerospace Conference, Big Sky, MT, USA, 4–11 March 2023; pp. 1–15.
14. Zhang, P.; Dai, W.; Niu, R.; Zhang, G.; Liu, G.; Liu, X.; Bo, Z.; Wang, Z.; Zheng, H.; Liu, C.; et al. Overview of the Lunar In Situ Resource Utilization Techniques for Future Lunar Missions. *Space Sci. Technol.* **2023**, *3*, 0037. [[CrossRef](#)]
15. Win, M.Z.; Scholtz, R.A. Ultra-wide bandwidth time-hopping spread-spectrum impulse radio for wireless multiple-access communications. *IEEE Trans. Commun.* **2000**, *48*, 679–689. [[CrossRef](#)]
16. Nikookar, H.; Prasad, R. *UWB Technologies*; Springer: Dordrecht, The Netherlands, 2009; pp. 117–133. [[CrossRef](#)]
17. Sahinoglu, Z.; Gezici, S.; Guvenc, I. *Ultra-Wideband Positioning Systems: Theoretical Limits, Ranging Algorithms, and Protocols*; Cambridge University Press: Cambridge, UK, 2008.
18. Fontana, R.J. *Recent Applications of Ultra Wideband Radar and Communications Systems*; Springer: Boston, MA, USA, 2002; pp. 225–234. [[CrossRef](#)]
19. Molisch, A.F.; Cassioli, D.; Chong, C.-C.; Emami, S.; Fort, A.; Kannan, B.; Karedal, J.; Kunisch, J.; Schantz, H.G.; Siwiak, K.; et al. A comprehensive standardized model for ultrawideband propagation channels. *IEEE Trans. Antennas Propag.* **2006**, *54*, 3151–3166. [[CrossRef](#)]
20. Akyildiz, I.F.; Jornet, J.M.; Han, C. Terahertz band: Next frontier for wireless communications. *Phys. Commun.* **2016**, *18*, 292–318. [[CrossRef](#)]
21. Verdu, S. *Multiuser Detection*; Cambridge University Press: Cambridge, UK, 1998.
22. Skrzypczak, A.; Palicot, J.; Siohan, P. Ofdm/oqam modulation for efficient dynamic spectrum access. *Int. J. Commun. Netw. Distrib. Syst.* **2012**, *8*, 247–266. [[CrossRef](#)]
23. Schulman, J.; Wolski, F.; Dhariwal, P.; Radford, A.; Klimov, O. Proximal Policy Optimization Algorithms. *arXiv* **2017**, arXiv:1707.06347.
24. Russell, S.J.; Norvig, P. *Artificial Intelligence: A Modern Approach*, 4th ed.; Pearson Education, Inc.: London, UK, 2021.
25. Huo, Z.; Zhang, L.; Zeng, Z.; Li, J.; Li, L.; Liu, C. Simulation of Lunar Comprehensive Substructure with Fracture and Imaging of Later LPR Data from Chang'e-4 Mission. *IEEE Trans. Geosci. Remote Sens.* **2023**, *61*, 5104611. [[CrossRef](#)]

Disclaimer/Publisher's Note: The statements, opinions and data contained in all publications are solely those of the individual author(s) and contributor(s) and not of MDPI and/or the editor(s). MDPI and/or the editor(s) disclaim responsibility for any injury to people or property resulting from any ideas, methods, instructions or products referred to in the content.